^{11}C-sorafenib and ^{15}O-H$_2$O PET for early evaluation of sorafenib therapy

Lemonitsa H. Mammatas[1,2], Maqsood Yaqub[3], N. Harry Hendrikse[3], Otto S. Hoekstra[3], Richard J. Honeywell[1], Robert C. Schuit[3], Martijn Meijerink[3], Lothar A. Schwarte[4], Godefridus J. Peters[1,5], Henk M.W. Verheul[1,6], Adriaan A. Lammertsma[3], C. Willemien Menke-van der Houven van Oordt[1]

[1]Department of Medical Oncology, Amsterdam UMC, location VUmc, Amsterdam, The Netherlands.

[2]Department of Medical Oncology, Reinier de Graaf Hospital, Delft, The Netherlands.

[3]Department of Radiology and Nuclear Medicine, Amsterdam UMC, location VUmc, Amsterdam, The Netherlands.

[4]Department of Anesthesiology, Amsterdam UMC, location VUmc, Amsterdam, The Netherlands.

[5]Department of Biochemistry, University of Gdansk, Gdansk, Poland.

[6]Department of Medical Oncology, Radboud University Medical Center, Nijmegen, The Netherlands.

Correspondence: C.W. Menke-van der Houven van Oordt, Amsterdam UMC, location VUmc, de Boelelaan 1117, 1081 HV Amsterdam, The Netherlands. Tel: (+31)20-4441050. Fax: (+31)20-4444355. E-mail: c.menke@amsterdamumc.nl

First Author: L.H. Mammatas, Amsterdam UMC, location VUmc, de Boelelaan 1117, 1081 HV Amsterdam, The Netherlands. Tel: (+31)20-4441050. Fax: (+31)20-4444355. E-mail: l.mammatas@amsterdamumc.nl

ABSTRACT

Purpose: Sorafenib leads to clinical benefit in a subgroup of patients, while all are exposed to potential toxicity. Currently, no predictive biomarkers are available. The purpose of this study was to evaluate whether ^{11}C-sorafenib and ^{15}O-H$_2$O PET have potential to predict treatment efficacy.

Methods: In this prospective exploratory study, 8 patients with advanced solid malignancies and an indication for sorafenib treatment were included. Microdose ^{11}C-sorafenib and perfusion ^{15}O-H$_2$O dynamic PET scans were performed before and after two weeks of sorafenib therapy. The main objective was to assess whether tumor ^{11}C-sorafenib uptake predicts sorafenib concentrations during therapy in corresponding tumor biopsies measured with liquid chromatography tandem mass spectrometry (LC-MS/MS). Secondary objectives included the association of ^{11}C-sorafenib PET, perfusion ^{15}O-H$_2$O PET and sorafenib concentrations after therapeutic dosing with response.

Results: ^{11}C-sorafenib PET did not predict sorafenib concentrations in tumor biopsies during therapy. In addition, sorafenib plasma and tumor concentrations, were not associated with clinical outcome in this exploratory study. Higher ^{11}C-sorafenib accumulation in tumors at baseline and day 14 of treatment showed association with poorer prognosis and was correlated with tumor perfusion (r_s = 0.671, P = 0.020). Interestingly, a decrease in tumor perfusion measured with ^{15}O-H$_2$O PET after only 14 days of therapy showed an association with response, with a decrease in tumor perfusion of 56% ± 23% (mean ± SD) versus 18% ± 32% in patients with stable and progressive disease, respectively.

Conclusion: Microdose ^{11}C-sorafenib PET did not predict intratumoral sorafenib concentrations after therapeutic dosing, but the association between a decrease in tumor perfusion and clinical benefit warrants further investigation.

INTRODUCTION

Since the discovery of Rapidly Accelerated Fibrosarcoma (RAF) kinases in 1983 as oncoproteins involved in cancer proliferation, migration and survival, protein kinase inhibitors have been developed in an attempt to inhibit these RAF kinases (*1*). Sorafenib was the first clinically successful RAF inhibitor (*2*). The molecular properties of sorafenib (~ 637 Daltons) enable diffusion and transporter mediated uptake into the cell. Sorafenib competes with adenosine triphosphate in order to occupy the hydrophobic pocket directly adjacent to its binding site, thereby trapping protein kinases in an inactive state (*3*). Apart from RAF kinases, sorafenib has shown affinity for multiple other protein kinases, thereby suppressing angiogenesis and inducing apoptosis (*4*). Sorafenib has been approved for treatment of locally advanced and metastatic hepatocellular carcinoma, renal cell carcinoma and iodine-refractory differentiated thyroid carcinoma (*5-7*). However, response to sorafenib is variable, resulting in clinical benefit for only a subgroup of patients, while all are exposed to potential toxicity (*5-7*). Most common side effects include gastrointestinal symptoms, fatigue, and (hand-foot) skin reactions (*5-7*). Currently, no biomarkers are available to identify which patients are likely to benefit from sorafenib.

The response to sorafenib is thought to be directly related to drug concentrations in tumor tissue (*8*). Non-invasive quantification of drug uptake in tumors and normal tissues at different time points using positron emission tomography (PET) imaging may provide insight in tissue pharmacokinetics in relation to therapeutic effects. For some protein kinase inhibitors, such as [^{11}C]erlotinib PET, this approach already has shown clinical relevance (*9*). PET is a highly sensitive method to detect tracer concentrations in the body at the lower picomolar range (10^{-12} mol/L) (*10*). This enables the use of a microdose drug tracer, i.e. a drug dose < 1% of the expected pharmacologically active concentration, avoiding toxicity of the studied drug (*11*). The tracer ^{11}C-sorafenib has been developed without changing the molecular structure of the drug itself (*12*). In mice, ^{11}C-sorafenib PET showed tumor uptake in the RAF-expressing human renal cell carcinoma xenograft RXF393 (*12*).

The purpose of the present study was to explore whether ^{11}C-sorafenib uptake in tumors can be used as a potential biomarker for treatment efficacy. The primary objective was to assess whether microdose ^{11}C-sorafenib PET at baseline or a change in uptake after 14 days of treatment (steady state), could predict sorafenib concentrations after therapeutic dosing as measured in corresponding tumor biopsies. Secondary objectives were to investigate the effect of tumor perfusion on ^{11}C-sorafenib delivery and to assess the anti-angiogenic effects of sorafenib on tumor perfusion. Finally, ^{11}C-sorafenib uptake and sorafenib concentrations in tumors, together with tumor perfusion (changes), were related to patient outcome.

MATERIALS AND METHODS

Study Design

This prospective exploratory study, with a planned sample size of n = 8, was conducted at the Amsterdam UMC, location VUmc, The Netherlands. Patients underwent dynamic microdose ^{11}C-sorafenib PET scans before ('baseline') and after two weeks of treatment with sorafenib 400 mg twice daily ('on treatment') when steady state levels of sorafenib were reached (*13*). Within 2 hours of the on treatment ^{11}C-sorafenib PET scan, a tumor biopsy and a venous blood sample were taken to measure (unlabeled) steady state sorafenib concentrations during therapy. Prior to each ^{11}C-sorafenib PET scan, a dynamic ^{15}O-H_2O PET scan was performed to measure tumor perfusion (Figure 1). For all patients, sorafenib treatment was continued until progressive disease, severe toxicity, or refusal by the patient.

Patient Population

Adult patients with a histologically confirmed, metastatic solid malignancy accessible for tumor biopsy, who were eligible for standard palliative treatment with sorafenib, were included i.e.

hepatocellular carcinoma, renal cell carcinoma and iodine-refractory differentiated thyroid carcinoma (other in- and exclusion criteria are shown in Supplement Table 1).

The study was approved by the Medical Ethics Review Committee of Amsterdam UMC, location VUmc (NCT02111889) and all subjects signed a written informed consent.

Tracer Synthesis

^{11}C-sorafenib and ^{15}O-H$_2$O were produced according to good manufacturing practice guidelines, as described previously (*12,14*). Carbon-11 was incorporated in the molecular structure of sorafenib at the terminal methylamide position.

PET Scanning

Scans were performed using a Gemini TF-64 PET-CT scanner (Philips Medical Systems, Best, The Netherlands) with an 18.4 cm axial field of view, divided into 45 contiguous planes. Patients received two venous catheters (for tracer injection and manual venous sampling, respectively) and an indwelling catheter in the radial artery for continuous arterial blood sampling during PET/CT. Patients were positioned supine on the scanner bed. Elastic body-restraining bandages were used to minimize movement during PET-CT scanning. A CT based topogram was performed to determine that both tumor and left ventricle were within the field of view of the scanner. Next, a 10 minutes dynamic scan was performed, starting at the time of an intravenous injection of ~370 MBq ^{15}O-H$_2$O (5 mL at a rate of 0.8 mL·sec^{-1}, followed by a 35 mL saline flush at a rate of 2.0 mL·sec^{-1}). Finally, a 60 minutes dynamic scan was acquired, starting at the time of an intravenous injection of ~370 MBq ^{11}C-sorafenib (5 mL at a rate of 0.8 mL·sec^{-1}, followed by a 35 mL saline flush at a rate of 2.0 mL·sec^{-1}). A 30 mAs low-dose CT scan was performed between ^{11}C-sorafenib and ^{15}O-H$_2$O dynamic PET scans for attenuation correction and segmentation purposes.

6

Using the three-dimensional row action maximum likelihood reconstruction algorithm (3D RAMLA), ^{15}O-H$_2$O scans were reconstructed into 26 frames with increasing duration (1 x 10, 8 x 5, 4 x 10, 2 x 15, 3 x 20, 2 x 30 and 6 x 60 s). ^{11}C-sorafenib scans were reconstructed into 36 frames (1 x 10, 8 x 5, 4 x 10, 3 x 20, 5 x 30, 5 x 60, 4 x 150, 4 x 300 and 2 x 600 sec). All data were normalized and corrected for dead time, decay, randoms, scatter and attenuation. Resulting PET images consisted of 128 x 128 x 90 isotropic voxels, with 4 x 4 x 4 mm^3 voxel size, and a final resolution of 5 mm FWHM.

Blood Sampling

During ^{15}O-H$_2$O and ^{11}C-sorafenib scans, arterial blood was withdrawn continuously at a rate of 300 mL·h^{-1} for the first five minutes and 150 mL·h^{-1} thereafter until the end of the scan, using an online detection system (Comecer, Joure, The Netherlands) (*15*). In addition, 7 mL arterial and venous samples were collected manually in lithium heparine containing tubes at 5, 7 and 9 minutes after injection of ^{15}O-H$_2$O and at 5, 10, 20, 30, 40 and 60 minutes after injection of ^{11}C-sorafenib. After each sample the line was flushed with 2 mL saline. These venous samples were used for measuring plasma-to-whole blood ratios, and for measuring plasma fractions of parent ^{11}C-sorafenib and radiolabeled metabolites. The arterial samples were used for calibration of the continuous arterial input curve. Because of the invasive character of an arterial catheter, a non-invasive image derived input function (IDIF) was also investigated (Supplement Figure S1).

Blood Radioactivity Concentrations of Tracer and Metabolites

Whole blood and plasma radioactivity concentrations of the parent drug and its radiolabeled metabolites were determined in the blood samples using a well-counter, cross-calibrated against the PET scanner (Supplement Table S2).

Volume of Interest Definition

Volume of interests (VOIs) of tumor lesions were defined manually on low dose CT scans, avoiding large blood vessels and normal liver tissue. In addition to the complete tumor volume, a separate VOI was defined for the rim of each tumor lesion using 2 voxels from the outer border of the tumor contour for comparison with tracer uptake in the whole tumor VOI, as central tumor necrosis may affect tracer uptake. Next, low-dose CT VOIs were projected onto corresponding dynamic PET images to generate time-activity curves (TAC) for ^{11}C-sorafenib and ^{15}O-H_2O. In addition, VOIs were defined on normal organs for ^{11}C-sorafenib biodistribution (*16*).

Analysis of Tumor Perfusion

Tumor perfusion (F in mL/cm^3/min) was obtained by fitting each ^{15}O-H_2O TAC to the single-tissue compartment model in combination with the arterial input function, as described previously (*17*). This model was implemented in Matlab R2017B software (MathWorks, Natick, USA).

Biodistribution of ^{11}C-sorafenib in Healthy Tissues

The biodistribution of ^{11}C-sorafenib in healthy tissues was measured during the 40-60 minutes interval of the dynamic PET scan and expressed as the mean standardized uptake value (SUV$_{mean}$), which is routinely used for evaluating the biodistribution in normal tissues (*18*).

[11]C-sorafenib Pharmacokinetics in Tumors

Tumor TACs derived from ^{11}C-sorafenib scans at baseline and after 14 days therapy were fitted to three different compartment models (i.e. 1-tissue, irreversible 2-tissue and reversible 2-tissue models) using the arterial plasma input function, corrected for radiolabeled metabolites. All models included a blood volume parameter to account for intravascular activity. The optimal model for describing the TAC data was selected based on Akaike Information and Schwartz Criteria (*19,20*).

Sorafenib Concentrations in Tumor and Plasma during Therapy

Using 14-16 Gauge biopsy needles, experienced intervention radiologists obtained tumor biopsies. In case of central necrosis, as seen on CT, samples were taken from the rim of the tumor. Samples were snap frozen within 1 minute of the biopsy, followed by storage under -80 °C conditions. Both plasma and tumor tissue samples were obtained within 2 hours of the on treatment ^{11}C-sorafenib PET scan. Liquid chromatography tandem mass spectrometry (LC-MS/MS) was used as a reference method to measure sorafenib concentrations, as described previously (*21*).

Safety and Response Evaluation

Safety evaluations were performed in all patients with grading of adverse events according to the National Cancer Institute Common Terminology Criteria for Adverse Events, version 4.0. Tumor response evaluation was performed every 2 months during sorafenib therapy according to Response Evaluation Criteria in Solid Tumors (RECIST) version 1.1 (*22*).

Statistical Analysis

Statistical analyses were performed using SPSS software for Windows version 22.0 (SPSS Inc. Chicago, USA). Tumor uptake of ^{11}C-sorafenib (both at baseline and on treatment PET scan) was compared with corresponding tumor and plasma sorafenib concentrations and with the calculated tumor-to-plasma concentration ratio of sorafenib after therapeutic dosing. PET measures are presented as mean ± SD. Correlations were explored using Spearman's correlation coefficient (r_s). The Wilcoxon signed rank test was used to compare PET measures before and after 14 days of sorafenib treatment, and to compare whole tumor and tumor rim values. A 2-tailed probability value of < 0.05 was considered significant.

RESULTS

Patient Characteristics

Eight patients were included (Table 1) between September 2013 and November 2015. There were no side effects during tracer injection or imaging procedures. Patients received 100% of the therapeutic dose during sorafenib treatment, except for patient 4. This patient had to end study participation within 2 weeks of treatment as a result of unexpected rapid clinical progression. In the other patients at least one contrast-enhanced CT scan was obtained for response evaluation. Five patients had progressive disease at first evaluation and two patients had stable disease for 20 and 44 weeks, respectively.

Biodistribution of ^{11}C-sorafenib

The highest ^{11}C-sorafenib accumulation was in the liver (SUV_{mean} 10.4 ± 3.3 at baseline and 6.4 ± 1.6 on treatment), whereas concentrations in skin were lowest (SUV_{mean} 0.3 ± 0.1 at baseline and 0.01 ± 0.01 on treatment) (Figure 2).

Comparison of ^{11}C-sorafenib uptake at baseline with that on treatment showed the largest differences in the liver with an SUV_{mean} decrease from 10.4 to 6.4 (P = 0.018) and in blood with an SUV_{mean} increase from 2.3 to 3.6 (P = 0.018).

No association was seen between the biodistribution of ^{11}C-sorafenib and treatment related toxicities.

Quantitative Analysis of ^{11}C-sorafenib Uptake in Tumors

A total of 15 lesions could be evaluated. Tumor volumes were highly variable, with a median size of 10 cm^3 and range of 4-2527 cm^3. Patient 4 only had a baseline ^{11}C-sorafenib scan due to early clinical deterioration.

A PET tracer dose of 347 ± 66 MBq (mean ± SD) ^{11}C-sorafenib was given with a specific activity of 35350 ± 9929 MBq/μmol sorafenib. As the molecular weight of sorafenib is 464.8

μg/μmol this corresponded with 4.9 ± 1.6 μg of unlabeled sorafenib. After injection, ^{11}C-sorafenib was quite stable, with only < 5% labeled metabolites formed during the 60 minutes scan. The reversible 2-tissue compartment model with four rate constants and additional blood volume parameter best described ^{11}C-sorafenib tumor kinetics (Supplement Figure S2). Therefore, the total volume of distribution (V_T) = $K_1/k_2*(1+k_3/k_4)$ was used as outcome parameter, which represents the tumor-to-plasma ratio of ^{11}C-sorafenib at equilibrium.

At baseline, 3/8 patients had a tumor V_T > 1, i.e. ^{11}C-sorafenib accumulation in the tumor was higher than in plasma (Figure 3). After 14 days of treatment, no patients were left with a tumor V_T > 1. Overall, tumor V_T values of ^{11}C-sorafenib were higher at baseline than at day 14 of treatment (0.68 ± 0.55 versus 0.29 ± 0.20, P = 0.007).

No significant differences in ^{11}C-sorafenib V_T were established between whole tumor and outer tumor rim (P = 0.944 at baseline and P = 0.138 at day 14). In addition, total tumor volume was not correlated with the amount of tracer uptake (r_s = 0.196, P = 0.483 at baseline and r_s = -0.134, P = 0.713 at day 14). Surprisingly, patients with clinical benefit had a lower tumor ^{11}C-sorafenib V_T in comparison to patients with progressive disease at baseline (0.34 ± 0.08 versus 0.92 ± 0.61) as well as after 14 days of treatment (0.13 ± 0.05 versus 0.37 ± 0.18) (Figure 4 A and 4B). In contrast, the percentage decrease in ^{11}C-sorafenib V_T between baseline and on treatment scans was not associated with clinical outcome (stable disease -58% ± 26% versus progressive disease -34% ± 55%).

Comparison of LC-MS/MS and ^{11}C-sorafenib PET Results

Sorafenib concentrations in tumor biopsies and plasma after two weeks of treatment as measured using LC-MS/MS are presented in Table 1. In plasma, the median sorafenib concentration was 6680 μg·L^{-1} (range: 4860-9610 μg·L^{-1}). The median sorafenib concentration in tumor biopsies was 5700 μg·L^{-1} (range: 3000-13400 μg·L^{-1}), which was lower than in plasma in 4 out of 8 patients. There was no correlation between plasma and tumor sorafenib concentrations

($r_s = 0.607$, $P = 0.148$). PET derived tumor ^{11}C-sorafenib V_T both at baseline and during therapy were not correlated with corresponding LC-MS/MS measured sorafenib concentrations in tumor biopsies ($r_s = -0.429$, $P = 0.337$ at baseline and $r_s = -0.250$, $P = 0.589$ at day 14) (Figure 5A). In addition, the calculated tumor-to-plasma concentration ratio of sorafenib after therapeutic dosing was not related to ^{11}C-sorafenib V_T (baseline as well as day 14 $r_s = -0.357$, $P = 0.432$) (Figure 5B). Also, the percentage difference of V_T between baseline and on treatment PET were not correlated with sorafenib concentrations in tumor biopsies ($r_s = -0.500$, $P = 0.267$), nor with the calculated tumor-to-plasma concentration ratio of sorafenib after therapeutic dosing ($r_s = -0.321$, $P = 0.498$). Moreover, plasma and tumor concentrations of sorafenib measured with LC-MS/MS during treatment were not associated with treatment outcome (plasma concentrations: 8245 µg/L ± 1930 µg/L versus 6807 µg/L ± 1483 µg/L and tumor concentrations: 8725 µg/L ± 4278 µg/L versus 7294 µg/L ± 5486 µg/L for stable versus progressive disease, respectively).

Tumor Perfusion Effects Measured using ^{15}O-H$_2$O PET

Tumor perfusion, measured using ^{15}O-H$_2$O PET, at baseline could be compared with that after 14 days of treatment in five out of eight patients. In the other patients only one ^{15}O-H$_2$O PET scan was performed as a result of technical problems (n = 2) or early study dropout (n = 1). Higher perfusion of the tumor rim at baseline and after 14 days of treatment was associated with higher ^{11}C-sorafenib V_T in the tumor (baseline $r_s = 0.671$, $P = 0.020$ and day 14 $r_s = 0.641$, $P = 0.025$), (Figure 6A). However, no significant correlation between ^{11}C-sorafenib uptake and total tumor perfusion at baseline and after 14 days of treatment was observed (baseline $r_s = 0.574$, $P = 0.056$ and day 14 $r_s = 0.485$, $P = 0.058$).

Analysis of tumor perfusion and clinical response revealed that patients with stable disease had larger decrease in total tumor perfusion (56% ± 23%) after 14 days of sorafenib treatment than patients with progressive disease (18% ± 32%) (Figure 6B).

DISCUSSION

To the best of our knowledge, this is the first clinical study directly comparing tracer uptake with drug concentrations after therapeutic dosing measured with LC-MS/MS in corresponding tumor biopsies. In contrast to expectations, this study showed that sorafenib concentrations in tumors during treatment could not be predicted by microdose ^{11}C-sorafenib PET. Both LC-MS/MS and PET are very accurate for the quantification of drug concentrations, with low test-retest variability in the range of 5-10% (*10,21,23,24*). However, there are biopsy and tracer dependent factors that may explain the observed discrepancies between LC-MS/MS and PET.

Biopsies only provide one sample of the tumor lesion. In case of intratumor heterogeneity this may lead to an under- or overestimation of sorafenib concentrations in the whole tumor. Overall, no significant intralesional heterogeneity of ^{11}C-sorafenib uptake between the whole tumor and its outer rim was established in this study. However, in larger tumors, regional differences in ^{11}C-sorafenib uptake were seen(Figure 3), supporting sample effects as a potential contributing factor to the discrepancies observed between LC-MS/MS and PET.

Another reason for discrepancies between LS/MS-MS and PET may be tracer dependent. Linearity in tumor pharmacokinetics, in other words dose proportionality, between microdose ^{11}C-sorafenib and standard dose sorafenib therapy was not observed in this study (Table 1). Non-linearity has been reported in 27% of the ascending drug dose studies by comparison of plasma drug concentrations, which can be due to the levels of drug transporters, metabolic enzymes and drug-target occupation (*25,26*).

First, drug transporting systems may become (partially) saturated after (prolonged) exposure to therapy in comparison to the tracer dose. Sorafenib is a substrate for organic anion and cation transporters, but uptake mostly depends on passive diffusion into cells (*27,28*). In addition, sorafenib is a substrate for efflux transporters, in particular breast cancer resistance protein (BCRP/ABCG2) and P-glycoprotein (P-gp/ABCB1). Sorafenib has demonstrated capacity to inhibit BCRP and P-gp in a dose-dependent manner (*29,30*). This could potentially result in less

tumor efflux of higher concentrations sorafenib. However, the affinity of sorafenib for these efflux transporters has shown to be weak and therefore tumor accumulation is not likely influenced by transporter-mediated alterations (*27*). The ^{11}C-sorafenib V_T in this study, which did not increase after 14 days of treatment, was consistent with this (Table 1).

Second, sorafenib is metabolized in the liver by uridine diphosphoglucose-glucuronosyltransferase 1A9 (UGT1A9) to sorafenib glucuronide and by CYP3A4 to the active metabolite sorafenib N-oxide (*31*). Saturation of these enzymes could add to the non-linearity. ^{11}C-sorafenib accumulated predominantly in the liver, however metabolite release to the bloodstream was very low (< 5%) as a result of rapid biliary excretion (*31*). Although therapeutic administration of sorafenib significantly reduced tracer uptake in the liver (P = 0.018) and increased available ^{11}C-sorafenib in the blood pool (P = 0.018), this did not result in increased tumor accumulation of ^{11}C-sorafenib after 14 days. In fact, tracer uptake decreased in most tumor lesions at day 14 (P = 0.007), most probably caused by competition of the microdose with the much higher concentrations of unlabeled sorafenib after therapeutic dosing.

Finally, another potential cause for the different results between tracer uptake and sorafenib concentrations after therapy may consist of the complex drug-target binding characteristics of this multikinase inhibitor with fast reversible as well as slow (ir)reversible target binding sites. Previously, the target binding kinetics of sorafenib have shown to be slower than for sunitinib and lenvatinib for example and therefore the 1 hour scanning time may have been too short to reflect drug-target occupation after 14 days of continuous sorafenib treatment (*32,33*). Overall, sorafenib showed low accumulation in tumors. A recent study in mice also demonstrated that sorafenib had significantly less intratumoral drug accumulation in comparison with other anti-angiogenic drugs (*8*), which may in part be attributed to sorafenib 's higher protein bound fraction in blood (> 99%) and its strong binding affinity for albumin, as it is assumed that only the free (unbound) drug can induce a pharmacologic effect (*34,35*). In only 3 of the 8 patients ^{11}C-sorafenib accumulation was higher in tumors than in plasma, which was correlated with increased perfusion

14

of the tumor rim (for the whole tumor this was only borderline significant, presumably a result of central tumor necrosis).

Higher ^{11}C-sorafenib accumulation in tumors at baseline or after 14 days of sorafenib treatment was not related with treatment benefit. On the contrary, clinical benefit was associated with lower ^{11}C-sorafenib uptake in tumors, which may be a result of the lower tumor perfusion observed in these patients. This is a prognostic rather than a predictive imaging finding and in line with previous studies showing that higher expression of pro-angiogenic factors such as VEGF and VEGFR 1-3 and increased tumor vascularity were associated with poorer prognosis in patients with hepatocellular carcinoma, renal cell carcinoma and follicular thyroid carcinoma (*36-39*). Some other microdose drug tracers, such as ^{11}C-erlotinib and ^{11}C-docetaxel, showed that higher tracer accumulation in tumors was in fact correlated with treatment benefit (*9,40*). The tracer signal of ^{11}C-sorafenib is more complex as it binds to multiple pharmacological targets with different affinity and the signal may be dominated by some targets, while other targets with less affinity may lead to stronger anti-tumor effects and these target effects may also differ between different tumor types (*41,42*). In addition, neither LC-MS/MS measured sorafenib concentrations in plasma nor tumor biopsies during therapy were useful predictors of clinical response in this exploratory study. Possibly, because the current tumor concentrations achieved with sorafenib therapy already induce sufficient protein kinase inhibition (*42*). However, another explanation may be that tumor concentrations reached with the current therapeutic schedule are in fact too low, resulting in overall marginal clinical activity. Consequently, even higher tumor concentrations may be necessary to improve the anti-cancer effects of sorafenib. Preclinical and clinical studies have indeed shown that higher levels of sorafenib exposure, in comparison with the levels reached with standard sorafenib dosing, are associated with improved anti-tumor activity, but dose escalation is limited by the toxicity of sorafenib (*43-45*).

The current exploratory study showed preliminary evidence for the value of ^{15}O-H$_2$O PET in early response prediction to sorafenib treatment. After only 2 weeks of treatment, tumor blood

flow decreased more in patients with clinical benefit as compared with patients with progressive disease (56 versus 18%). Although these results are limited by the small cohort size of this study, it is in line with other angiogenesis inhibitors. For example, early reduction in tumor perfusion as shown with ^{15}O-H$_2$O PET was also associated with clinical benefit in patients treated with bevacizumab and sunitinib (*46,47*). Thus, early decrease in tumor perfusion may have predictive value for outcome of sorafenib treatment. Given the potential benefit for patients of early response prediction, this finding warrants further investigation.

CONCLUSION

In conclusion, microdose ^{11}C-sorafenib PET was not useful for the prediction of intratumoral sorafenib concentrations during treatment measured with LC-MS/MS. However, there was preliminary evidence for an association between a decrease in tumor perfusion after only 2 weeks of sorafenib therapy and clinical benefit. This warrants further investigation to assess its value as an early biomarker for sorafenib efficacy.

KEY POINTS

QUESTION: Do ^{11}C-sorafenib and ^{15}O-H$_2$O PET have value for early evaluation of sorafenib therapy in patients with advanced solid malignancies?

PERTINENT FINDINGS: In this prospective exploratory study, ^{11}C-sorafenib uptake in tumors at baseline and day 14 of treatment were not predictive for sorafenib concentrations after therapeutic dosing as measured in corresponding tumor biopsies using LC-MS/MS. There was preliminary evidence that a decrease in tumor perfusion measured with ^{15}O-H$_2$O PET after only 14 days of therapy correlated with clinical benefit, with a decrease in tumor perfusion of 56% ± 23% (mean ± SD) versus 18% ± 32% in patients with stable and progressive disease, respectively.

IMPLICATIONS FOR PATIENT CARE: Our results support that a larger prospective study is warranted to evaluate whether a decrease in tumor perfusion measured with ^{15}O-H$_2$O PET can indeed be used as an early therapeutic biomarker of sorafenib efficacy.

REFERENCES

1. Rapp UR, Goldsborough MD, Mark GE, et al. Structure and biological activity of v-raf, a unique oncogene transduced by a retrovirus. *Proc Natl Acad Sci U S A.* 1983;80:4218-4222.

2. Wilhelm S, Carter C, Lynch M, et al. Discovery and development of sorafenib: a multikinase inhibitor for treating cancer. *Nat Rev Drug Discov.* 2006;5:835-844.

3. Gotink KJ, Verheul HM. Anti-angiogenic tyrosine kinase inhibitors: what is their mechanism of action? *Angiogenesis.* 2010;13:1-14.

4. Wilhelm SM, Adnane L, Newell P, Villanueva A, Llovet JM, Lynch M. Preclinical overview of sorafenib, a multikinase inhibitor that targets both Raf and VEGF and PDGF receptor tyrosine kinase signaling. *Mol Cancer Ther.* 2008;7:3129-3140.

5. Escudier B, Eisen T, Stadler WM, et al. Sorafenib for treatment of renal cell carcinoma: Final efficacy and safety results of the phase III treatment approaches in renal cancer global evaluation trial. *J Clin Oncol.* 2009;27:3312-3318.

6. Llovet JM, Ricci S, Mazzaferro V, et al. Sorafenib in advanced hepatocellular carcinoma. *N Engl J Med.* 2008;359:378-390.

7. Brose MS, Nutting CM, Jarzab B, et al. Sorafenib in radioactive iodine-refractory, locally advanced or metastatic differentiated thyroid cancer: a randomised, double-blind, phase 3 trial. *Lancet.* 2014;384:319-328.

8. Torok S, Rezeli M, Kelemen O, et al. Limited Tumor Tissue Drug Penetration Contributes to Primary Resistance against Angiogenesis Inhibitors. *Theranostics.* 2017;7:400-412.

9. Bahce I, Smit EF, Lubberink M, et al. Development of [(11)C]erlotinib positron emission tomography for in vivo evaluation of EGF receptor mutational status. *Clin Cancer Res.* 2013;19:183-193.

10. Cunningham VJ, Pike VW, Bailey D, et al. A method of studying pharmacokinetics in man at picomolar drug concentrations. *Br J Clin Pharmacol.* 1991;32:167-172.

11. Mammatas LH, Verheul HM, Hendrikse NH, Yaqub M, Lammertsma AA, Menke-van der Houven van Oordt CW. Molecular imaging of targeted therapies with positron emission tomography: the visualization of personalized cancer care. *Cell Oncol (Dordr).* 2015;38:49-64.

12. Poot AJ, van der Wildt B, Stigter-van Walsum M, et al. [(1)(1)C]Sorafenib: radiosynthesis and preclinical evaluation in tumor-bearing mice of a new TKI-PET tracer. *Nucl Med Biol.* 2013;40:488-497.

13. Strumberg D, Clark JW, Awada A, et al. Safety, pharmacokinetics, and preliminary antitumor activity of sorafenib: a review of four phase I trials in patients with advanced refractory solid tumors. *Oncologist.* 2007;12:426-437.

14. Jackson JR, Dembowski BS, Ehrenkaufer RL, McIntyre E, Reivich M. [15O]H2O, [15O]O2 and [15O]CO gas production, monitoring and quality control system. *Appl Radiat Isot.* 1993;44:631-634.

15. Boellaard R, van Lingen A, van Balen SC, Hoving BG, Lammertsma AA. Characteristics of a new fully programmable blood sampling device for monitoring blood radioactivity during PET. *Eur J Nucl Med.* 2001;28:81-89.

16. Jansen BHE, Kramer GM, Cysouw MCF, et al. Healthy Tissue Uptake of (68)Ga-Prostate-Specific Membrane Antigen, (18)F-DCFPyL, (18)F-Fluoromethylcholine, and (18)F-Dihydrotestosterone. *J Nucl Med.* 2019;60:1111-1117.

17. de Langen AJ, Lubberink M, Boellaard R, et al. Reproducibility of tumor perfusion measurements using 15O-labeled water and PET. *J Nucl Med.* 2008;49:1763-1768.

18. Ilhan H, Lindner S, Todica A, et al. Biodistribution and first clinical results of (18)F-SiFAlin-TATE PET: a novel (18)F-labeled somatostatin analog for imaging of neuroendocrine tumors. *Eur J Nucl Med Mol Imaging.* 2020;47:870-880.

19. Akaike H. A new look at the statistical model identification. *IEEE transactions on automatic control.* 1974;19:716-723.

20.   Schwarz G. Estimating the dimension of a model. *The annals of statistics.* 1978;6:461-464.

21.   Honeywell R, Yarzadah K, Giovannetti E, et al. Simple and selective method for the determination of various tyrosine kinase inhibitors used in the clinical setting by liquid chromatography tandem mass spectrometry. *J Chromatogr B Analyt Technol Biomed Life Sci.* 2010;878:1059-1068.

22.   Eisenhauer EA, Therasse P, Bogaerts J, et al. New response evaluation criteria in solid tumours: revised RECIST guideline (version 1.1). *Eur J Cancer.* 2009;45:228-247.

23.   Widmer N, Bardin C, Chatelut E, et al. Review of therapeutic drug monitoring of anticancer drugs part two--targeted therapies. *Eur J Cancer.* 2014;50:2020-2036.

24.   Lammertsma AA. Forward to the Past: The Case for Quantitative PET Imaging. *J Nucl Med.* 2017;58:1019-1024.

25.   Bergstrom M. The Use of Microdosing in the Development of Small Organic and Protein Therapeutics. *J Nucl Med.* 2017;58:1188-1195.

26.   Bosgra S, Vlaming ML, Vaes WH. To Apply Microdosing or Not? Recommendations to Single Out Compounds with Non-Linear Pharmacokinetics. *Clin Pharmacokinet.* 2016;55:1-15.

27.   Hu S, Chen Z, Franke R, et al. Interaction of the multikinase inhibitors sorafenib and sunitinib with solute carriers and ATP-binding cassette transporters. *Clin Cancer Res.* 2009;15:6062-6069.

28.   Honeywell R, Hitzerd S, Kathmann I, J Peters G. Transport of six tyrosine kinase inhibitors: active or passive? *ADMET and DMPK.* 2016;4:23-34.

29.   Wei Y, Ma Y, Zhao Q, et al. New use for an old drug: inhibiting ABCG2 with sorafenib. *Mol Cancer Ther.* 2012;11:1693-1702.

30.   Gnoth MJ, Sandmann S, Engel K, Radtke M. In vitro to in vivo comparison of the substrate characteristics of sorafenib tosylate toward P-glycoprotein. *Drug Metab Dispos.* 2010;38:1341-1346.

31.   Vasilyeva A, Durmus S, Li L, et al. Hepatocellular Shuttling and Recirculation of Sorafenib-Glucuronide Is Dependent on Abcc2, Abcc3, and Oatp1a/1b. *Cancer Res.* 2015;75:2729-2736.

32.   Okamoto K, Ikemori-Kawada M, Jestel A, et al. Distinct binding mode of multikinase inhibitor lenvatinib revealed by biochemical characterization. *ACS Med Chem Lett.* 2015;6:89-94.

33.   Neumann L, von Konig K, Ullmann D. HTS reporter displacement assay for fragment screening and fragment evolution toward leads with optimized binding kinetics, binding selectivity, and thermodynamic signature. *Methods Enzymol.* 2011;493:299-320.

34.   Villarroel MC, Pratz KW, Xu L, Wright JJ, Smith BD, Rudek MA. Plasma protein binding of sorafenib, a multi kinase inhibitor: in vitro and in cancer patients. *Invest New Drugs.* 2012;30:2096-2102.

35.   Zhang D, Hop C, Patilea-Vrana G, et al. Drug Concentration Asymmetry in Tissues and Plasma for Small Molecule-Related Therapeutic Modalities. *Drug Metab Dispos.* 2019;47:1122-1135.

36.   Toyoda H, Kumuda T, Nakano S, et al. Significance of tumor vascularity as a predictor of long-term prognosis in patients with small hepatocellular carcinoma treated by percutaneous ethanol injection therapy. *J Hepatol.* 1997;26:1055-1062.

37.   Iakovlev VV, Gabril M, Dubinski W, et al. Microvascular density as an independent predictor of clinical outcome in renal cell carcinoma: an automated image analysis study. *Lab Invest.* 2012;92:46-56.

38.   Wong NA, Willott J, Kendall MJ, Sheffield EA. Measurement of vascularity as a diagnostic and prognostic tool for well differentiated thyroid tumours: comparison of different methods of assessing vascularity. *J Clin Pathol.* 1999;52:593-597.

39.   Rini BI, Michaelson MD, Rosenberg JE, et al. Antitumor activity and biomarker analysis of sunitinib in patients with bevacizumab-refractory metastatic renal cell carcinoma. *J Clin Oncol.* 2008;26:3743-3748.

40.   van der Veldt AA, Lubberink M, Mathijssen RH, et al. Toward prediction of efficacy of chemotherapy: a proof of concept study in lung cancer patients using [(1)(1)C]docetaxel and positron emission tomography. *Clin Cancer Res.* 2013;19:4163-4173.

41.   Karaman MW, Herrgard S, Treiber DK, et al. A quantitative analysis of kinase inhibitor selectivity. *Nat Biotechnol.* 2008;26:127-132.

42.   Labots M, Pham TV, Honeywell RJ, et al. Kinase Inhibitor Treatment of Patients with Advanced Cancer Results in High Tumor Drug Concentrations and in Specific Alterations of the Tumor Phosphoproteome. *Cancers (Basel).* 2020;12.

43.   Escudier B, Szczylik C, Hutson TE, et al. Randomized phase II trial of first-line treatment with sorafenib versus interferon Alfa-2a in patients with metastatic renal cell carcinoma. *J Clin Oncol.* 2009;27:1280-1289.

44.   Wang X, Zhang L, Goldberg SN, et al. High dose intermittent sorafenib shows improved efficacy over conventional continuous dose in renal cell carcinoma. *J Transl Med.* 2011;9:220.

45.   Mammatas LH, Zandvliet AS, Rovithi M, et al. Sorafenib administered using a high-dose, pulsatile regimen in patients with advanced solid malignancies: a phase I exposure escalation study. *Cancer Chemother Pharmacol.* 2020.

46.   de Langen AJ, van den Boogaart V, Lubberink M, et al. Monitoring response to antiangiogenic therapy in non-small cell lung cancer using imaging markers derived from PET and dynamic contrast-enhanced MRI. *J Nucl Med.* 2011;52:48-55.

47.   Scott AM, Mitchell PL, O'Keefe G, et al. Pharmacodynamic analysis of tumour perfusion assessed by 15O-water-PET imaging during treatment with sunitinib malate in patients with advanced malignancies. *EJNMMI Res.* 2012;2:31.
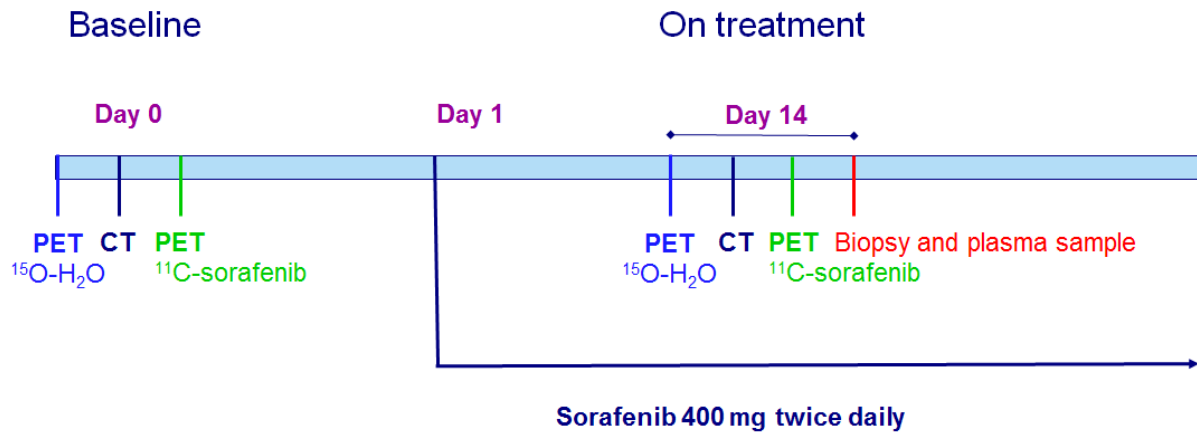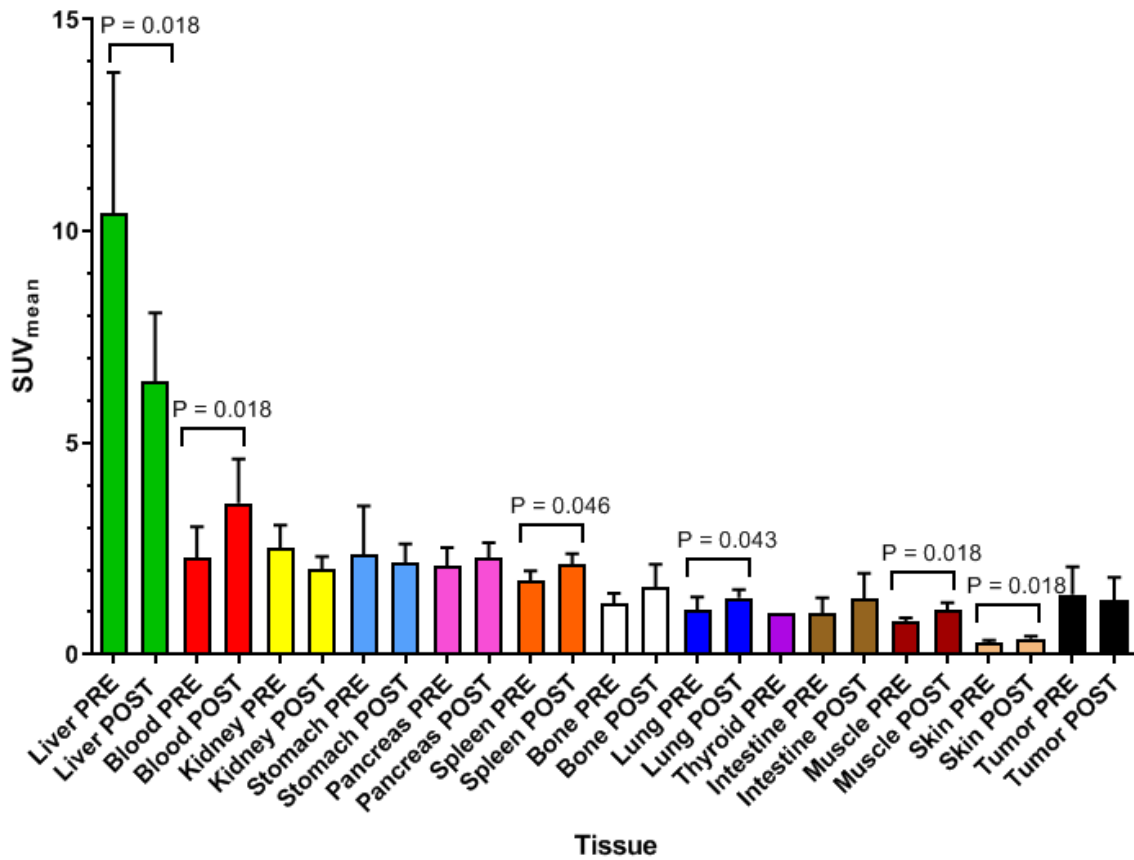
FIGURES

FIGURE 1. Study design.

FIGURE 2. Biodistribution of ^{11}C-sorafenib in different healthy tissues and tumor tissue. PRE = baseline, POST = after 14 days of sorafenib therapy.
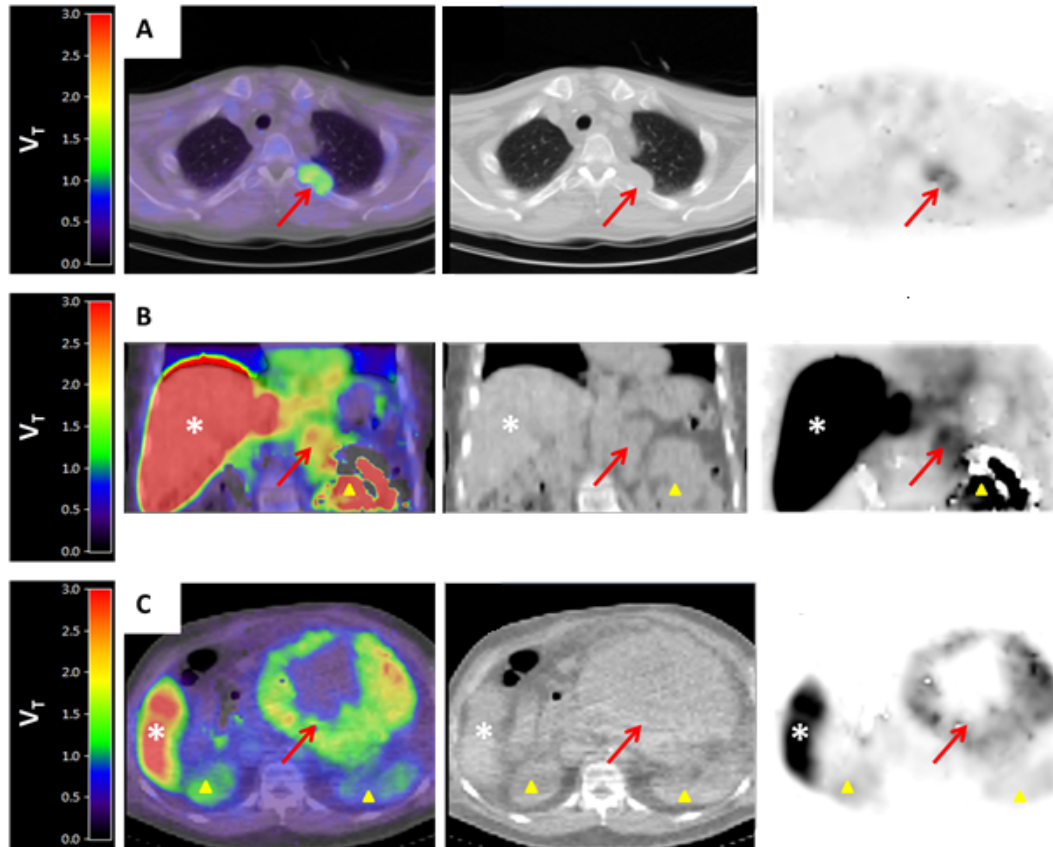
FIGURE 3. Fusion ^{11}C-sorafenib PET/CT (sum 40-60 min), low-dose CT and PET images from three patients showing ^{11}C-sorafenib uptake in tumor lesions (red arrows)). Patient A with hepatocellular carcinoma has a metastasis in the left costa 4, patient B with renal cell carcinoma has a metastasis in the left adrenal gland, and patient C with hepatocellular carcinoma has a large intra-abdominal metastasis. Physiologic uptake can be seen in the liver (white *) and kidneys (yellow Δ).
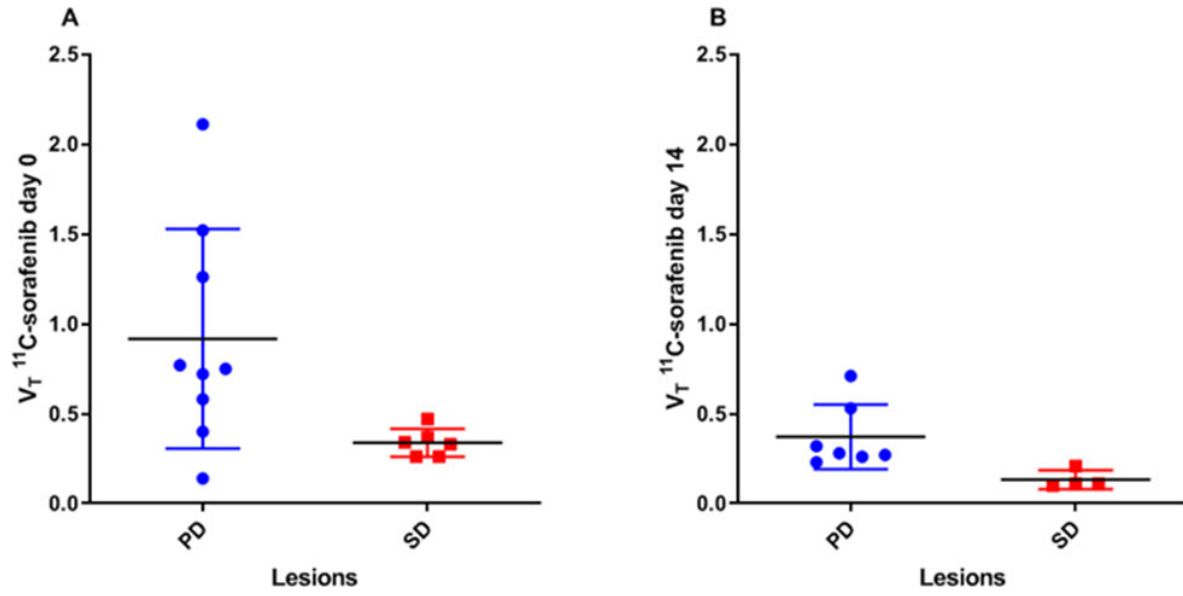
FIGURE 4. Tumor ^{11}C-sorafenib V_T on days 0 (A) and 14 (B) in lesions of patients with progressive (PD) and stable (SD) disease.
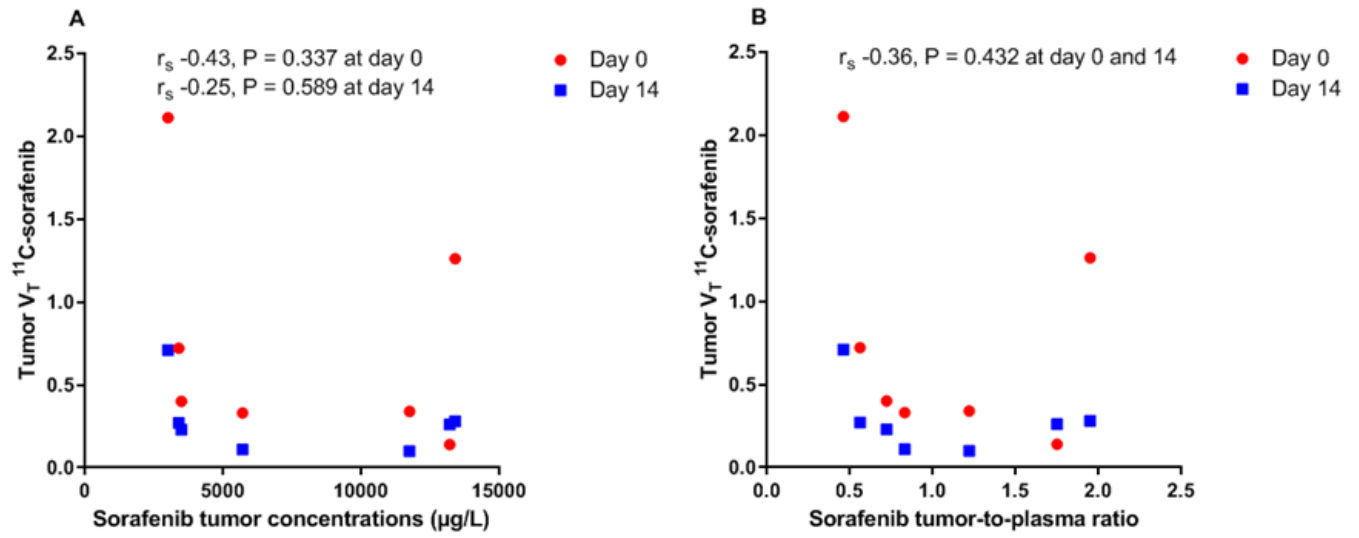
FIGURE 5. Correlation between tumor ^{11}C-sorafenib V_T values and the tumor sorafenib concentrations (A) and sorafenib tumor-to-plasma ratio (B) measured with LC-MS/MS.
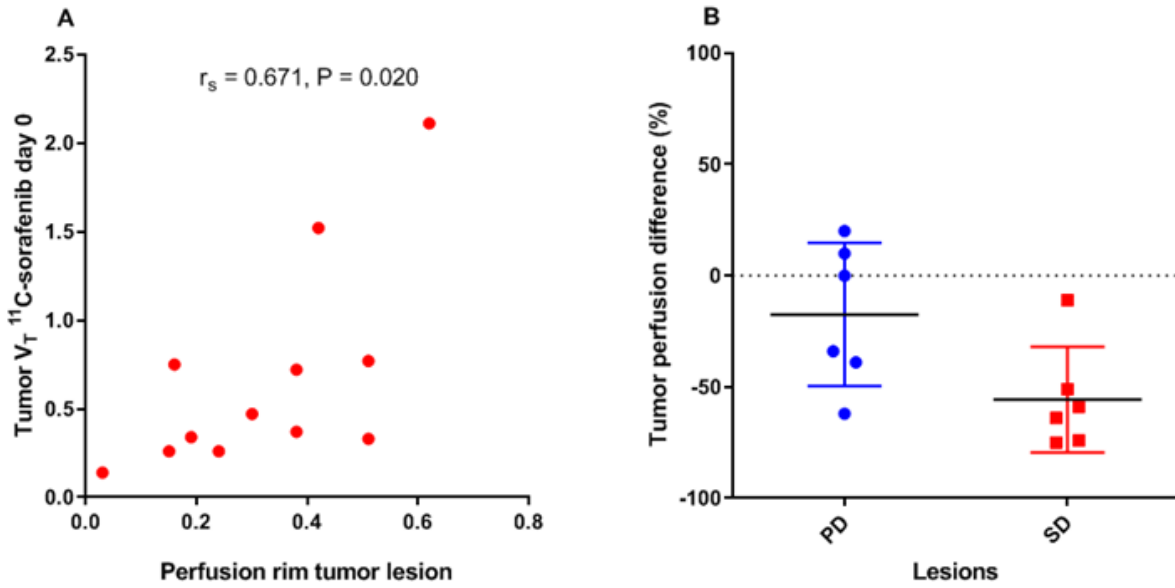
FIGURE 6. Correlation between tumor V_T values of ^{11}C-sorafenib and perfusion of the tumor rim (A). Tumor perfusion difference after 14 days of sorafenib treatment in patients with PD and SD (B).

TABLES

TABLE 1. Tumor and plasma sorafenib concentrations measured with LC-MS/MS and ^{11}C-sorafenib tumor V_T on day 0 and 14. DTC = differentiated thyroid carcinoma, RCC = renal cell carcinoma, HCC = hepatocellular carcinoma, PD = progressive disease, SD = stable disease.

Patient	Age (years)	Sex	Tumor	Biopsy site	Tumor (µg/L)	Plasma (µg/L)	Tumor-to-plasma ratio	V_T day 0	V_T day 14	Response
1	52	F	DTC	Skin	3390	6100	0.56	0.72	0.27	PD
2	55	M	RCC	Spleen	3480	4860	0.72	0.40	0.23	PD
3	59	M	RCC	Adrenal gland	5700	6880	0.83	0.33	0.11	SD
4	69	M	HCC	-	-	6180	-	1.52	-	PD
5	66	M	RCC	Lung	11750	9610	1.22	0.34	0.10	SD
6	60	F	RCC	Adrenal gland	3000	6490	0.46	2.11	0.71	PD
7	66	M	HCC	Liver	13400	6860	1.95	1.26	0.28	PD
8	59	M	RCC	Lung	13200	7550	1.75	0.14	0.26	PD

SUPPLEMENTAL MATERIAL

SUPPLEMENT TABLE S1
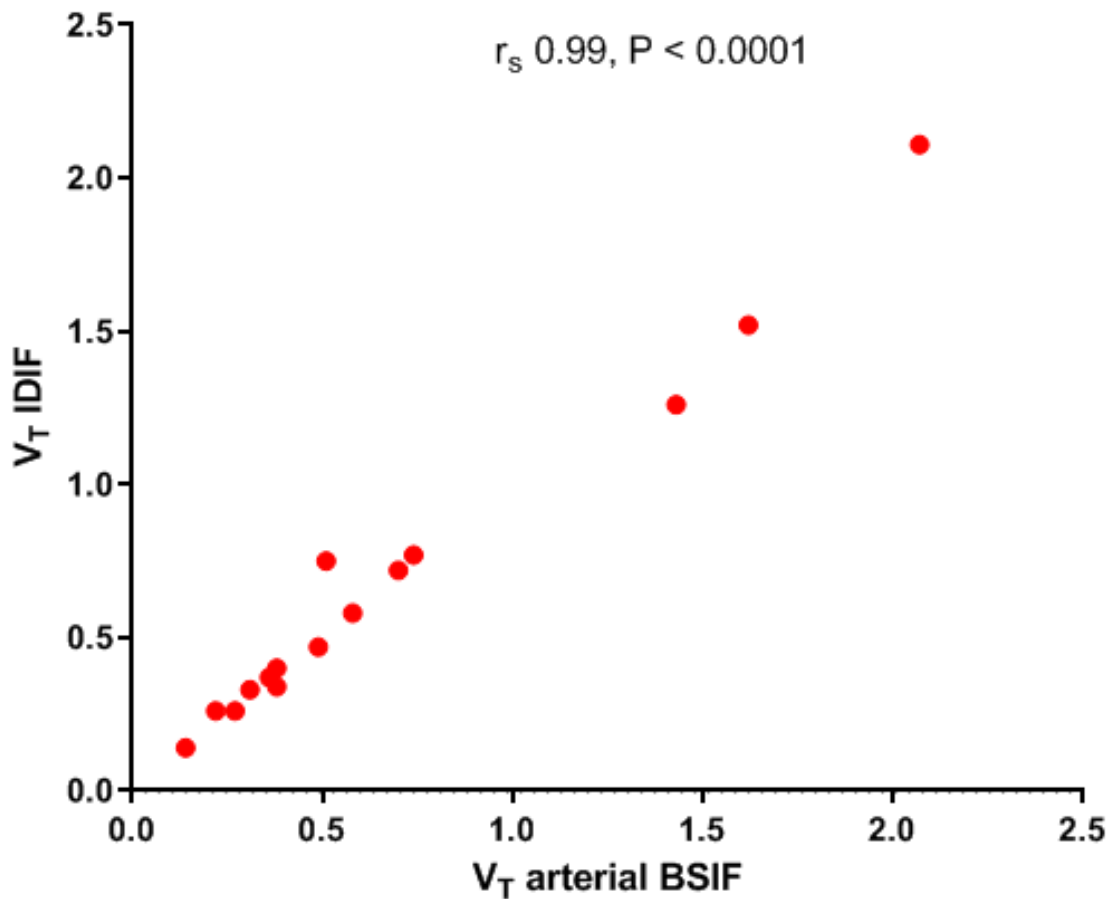
In- and exclusion criteria

Inclusion Criteria	**Exclusion Criteria**
- Eastern Cooperative Oncology Group performance status 0-2 - One or more extrahepatic tumor lesion(s) measurable according to RECIST version 1.1 (19) - Hemoglobin > 6.0 mmol/L - Absolute neutrophil count (ANC) > 1.5 x 10*9/L - Platelet count ≥ 100 x 10*9/L - Total bilirubin < 2 times the upper limit of normal (ULN) - Alanine aminotransferase (ALT) and aspartate aminotransferase (AST) < 2.5 x ULN or < 5x ULN in case of liver metastases (except for patients with hepatocellular carcinoma, then Child Pugh classification A-B) - Serum creatinine eGFR ≥ 50 mL/min	- Evidence of serious uncontrolled concomitant disease (such as infections, cardiovascular, pulmonary, skin and central nervous system diseases) - Major surgery < 28 - Thromboembolic events < 3 months

SUPPLEMENT TABLE S2

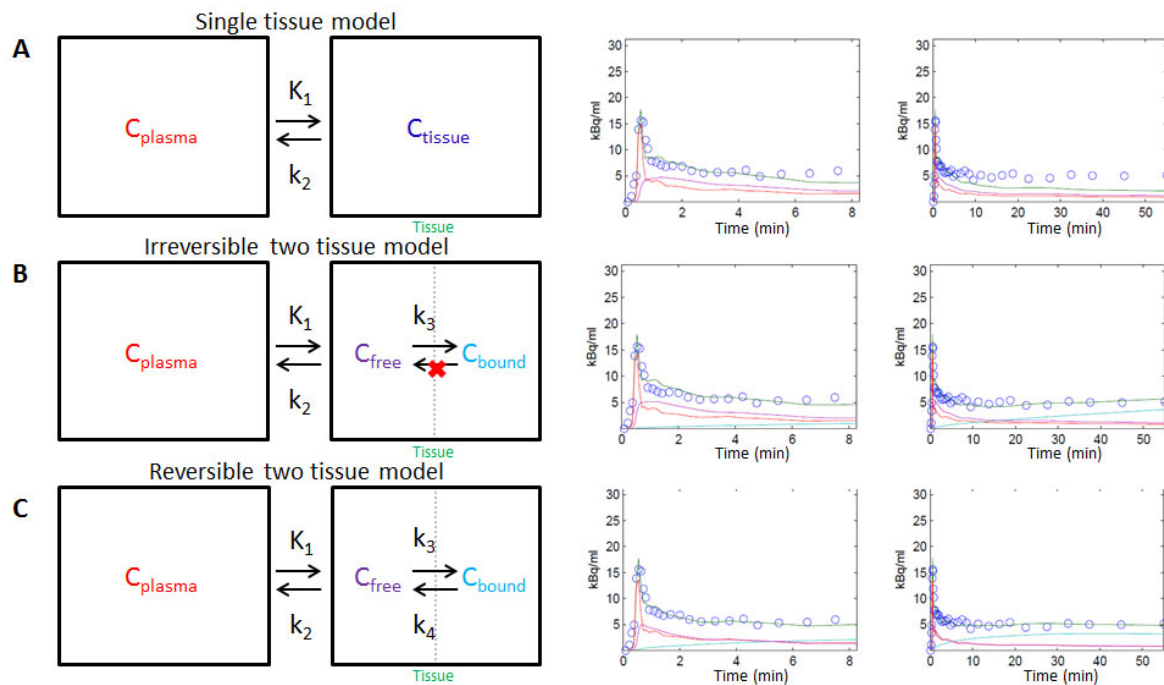Method to measure blood ^{11}C-sorafenib concentrations and metabolites

Method

- For ^{11}C-sorafenib, whole blood (0.5 mL) was weighed in duplicate and after centrifuging (5 minutes; 7°C; 4000 rpm)

- Plasma was collected and 0.5 mL was weighed in duplicate

- Solid phase extraction and high performance liquid chromatography (HPLC) were used to separate parent compound and radiolabeled metabolites and determine their fractions in the samples. Therefore, 1 mL plasma was diluted with 2 mL 0.15M HCl and transferred to a Waters Sep-Pak tC18 SPE column. The cartridge was washed with 5 mL of water and eluted with 1.5 mL of methanol

- This eluate was injected onto a Phenomenex Luna C18 5 µm 250 x 10 mm with a flow of 4 mL·min-1. The gradient system was a mixture of acetonitrile (A) and 0.1% trifluoroacetic acid (B) and was programmed as follows: t = 0 min 90% B, t = 9 min 20% B, t = 12 min 20% B, t = 15 min 90% B

- Fractions were collected and measured for radioactivity with a gamma-counter to generate an HPLC profile for ^{11}C-sorafenib and its labeled metabolites, respectively

SUPPLEMENT FIGURE S1.

Correlation between tumor V_T values of ^{11}C-sorafenib derived from the arterial blood sampler input function (BSIF) and those obtained using the less invasive image derived input function (IDIF). A VOI of 12 voxels in 3 planes was drawn in the left ventricle of the heart to measure ^{11}C-sorafenib concentrations in the blood pool to serve as IDIF. IDIFs were corrected for calibration, plasma to whole blood ratios and metabolites using the manual venous samples similarly to BSIF with arterial samples as described above. The non-invasive IDIF showed excellent correlation with the arterial BSIF, therefore IDIF can be used as a non-invasive alternative of BSIF to measure ^{11}C-sorafenib V_T in tumor lesions.

SUPPLEMENT FIGURE S2. Schematic diagram of the most frequently used compartment models: the single tissue compartment model (A), the irreversible two tissue compartment model (B) and the reversible two tissue compartment model (C). K_1 represents transport from plasma to tissue and k_2 from tissue to plasma and; k_3 and k_4 describe the exchange between free and bound tissue fractions. Typical ^{11}C-sorafenib tumor time-activity curves (blue circles) are fitted to plasma input (red line) according to these three models (green lines) and are shown for the peaks (0-8 minutes) and the complete time-activity curves (0-60 minutes). Akaike and Schwartz criteria showed preference for the reversible two tissue compartment model model in 68% of the tumor lesions, as compared with 25% for the 1-tissue model and 7% for the irreversible 2-tissue model.

GRAPHICAL ABSTRACT